N73-10251

NASA TECHNICAL MEMORANDUM

NASA TM X-2651

NASA TM X-2651

SYSTEM EFFICIENCY OF A MICROWAVE POWER TUBE WITH A MULTISTAGE DEPRESSED COLLECTOR

by James A. Dayton, Jr.

Lewis Research Center

Cleveland, Ohio 44135

NATIONAL AERONAUTICS AND SPACE ADMINISTRATION • WASHINGTON, D. C. • NOVEMBER 1972

1. Report No.	2. Government Accession No.	3. Recipient's Catalog No.
NASA TM X-2651		

4. Title and Subtitle	5. Report Date
SYSTEM EFFICIENCY OF A MICROWAVE POWER TUBE WITH A MULTISTAGE DEPRESSED COLLECTOR	November 1972
	6. Performing Organization Code
7. Author(s)	8. Performing Organization Report No.
James A. Dayton, Jr.	E-7057
	10. Work Unit No.
9. Performing Organization Name and Address	682-10
Lewis Research Center National Aeronautics and Space Administration Cleveland, Ohio 44135	11. Contract or Grant No.
	13. Type of Report and Period Covered
12. Sponsoring Agency Name and Address	Technical Memorandum
National Aeronautics and Space Administration Washington, D.C. 20546	14. Sponsoring Agency Code

15. Supplementary Notes

16. Abstract

The efficiencies of a microwave power tube with a multistage depressed collector and of the power supply driving the tube are computed. An analytical expression for the collector efficiency, which includes the effect of secondary emission and the radial component of velocity, is derived for a hypothetical current probability distribution function. In addition, collector efficiency is calculated with the aid of a digital computer for a specific current distribution. The efficiency of the power supply required to operate the tube in a space environment is estimated by using a simple parallel inverter system.

17. Key Words (Suggested by Author(s))	18. Distribution Statement
Microwave tubes Efficiency Power conditioning Toroidal transformer	Unclassified - unlimited

19. Security Classif. (of this report)	20. Security Classif. (of this page)	21. No. of Pages	22. Price*
Unclassified	Unclassified	28	$3.00

* For sale by the National Technical Information Service, Springfield, Virginia 22151

SYSTEM EFFICIENCY OF A MICROWAVE POWER TUBE WITH A MULTISTAGE DEPRESSED COLLECTOR

by James A. Dayton, Jr.

Lewis Research Center

SUMMARY

The efficiency of microwave transmitting power tubes and the power supplies which drive them are an important factor in the weight and cost of satellite communication systems. A promising technique for improving efficiency is the operation of the tube with a multistage depressed collector.

This report presents a method of estimating, with the aid of a digital computer, the efficiency of a tube equipped with a depressed collector when the electron current distribution is known. In addition, an analytical expression for tube efficiency which is based on a hypothetical current distribution is derived. Secondary emission and radial components of velocity are taken into account in these calculations. The biasing of collectors to achieve maximum efficiency is also discussed.

The efficiency of a simple power supply which could produce the necessary voltages and currents for operation of a microwave power tube with a multistage depressed collector is estimated and included in the program. The program does not design a complete operational power supply but does calculate transistor, transformer, and rectifier losses for a parallel converter. Losses in the filter and regulation circuits are estimated.

For the numerical examples presented herein, the first few depressed collector stages improve tube efficiency quite markedly; but after the sixth stage, efficiency is improved about 1 percent per stage.

INTRODUCTION

As communication satellites assume a greater share of the long-distance telephone and television traffic, the requirements for higher power output and higher efficiency become more pressing. The efficiency of the transmitting tube influences satellite weight in two ways: it directly determines both the size of the solar cell array needed to drive

the system and the size of the radiator needed to reject waste heat dissipated in the tube. It follows that, if the microwave transmitting tube is more efficient, the satellite can be lighter and, therefore, less expensive to build and launch.

Two methods of improving microwave tube efficiencies are being studied: raising electronic conversion efficiency and recovering energy from the spent electron beam by means of a depressed collector. The analysis of the latter method is the subject of this report.

The purpose of a depressed collector from the point of view of physical electronics is to collect the electrons in the spent beam at a potential such that their kinetic energy is very small, so that the energy wasted upon impact with the collector surface can be minimized. The same process may be described in terms of circuit analysis. In a properly designed microwave power tube, only a very small fraction of the beam current is intercepted at the anode or on the tube body and only this current need be supplied by the cathode power supply. The bulk of the power input to the tube then comes from the collector power supply, and most of this current is delivered at voltages much lower than the anode voltage. Hence, the improved efficiency of the tube.

The design of a multistage depressed collector has been the subject of a recent report by Kosmahl (ref. 1). Kavanagh, Alexovich, and Chomos (ref. 2) verified this design experimentally and obtained a collector efficiency of 57 percent for an electrostatically focused klystron with a seven-stage depressed collector. This result was obtained without refocusing the large lateral velocity spread present in the tube.

In other recently reported work on this subject Neugebauer and Mihran (ref. 3) were able to increase the efficiency of a 1-kilowatt, 750-megahertz klystron from 54.3 percent to 70.9 percent with a 10-stage, 60-percent-efficient depressed collector which utilized a refocusing solenoid. Okoshi, Chiu, and Matsuki (ref. 4) improved the efficiency of a 7-watt, 4-gigahertz traveling wave tube from 19 percent to 46 percent with a five-stage depressed collector.

This report studies the effect on collector efficiency of the number of depressed stages when the probability distribution of beam current is known. Some comment is made regarding the biasing of collectors for maximum improvement in tube efficiency. An analytic expression is derived for the case of a triangular current distribution, and an example is calculated by using a digital computer for a distribution calculated for a particular design. Both calculations considered the effects of secondary emission and the radial component of electron velocity. The calculations assume that the collector assembly is able to sort the electrons so that each electron strikes the collector which has the potential energy equal to or next below it in axial kinetic energy. The latter assumption implies that the entrance angles for the electrons in the spent beam are sufficiently well controlled, by beam refocusing if necessary, and that collector apertures are appropriately sized.

The efficiency of the power supply needed to drive the tube with a depressed collector is estimated for a parallel inverter with transistor switches and a single toroidal transformer with multiple secondary windings. The losses in the transistors, the transformer, and the rectifiers are computed; losses in the filters and the regulation circuits are only estimated. The power supply efficiency calculation is included in the computer program.

ANALYSIS OF TUBE EFFICIENCY

Collector Bias Voltage

The placement and biasing of depressed collector stages determines the resulting improvement in tube efficiency. When the probability distribution for beam current at the collector is known, the incremental improvement in the performance of the tube as a result of the addition of each successive stage may be estimated analytically.

In order to illustrate how this may be done, it is instructive to begin with an idealized current probability distribution function, as shown in figure 1(a), where the vertical axis represents the probability that electrons entering the collector region of an rf amplifier tube will have an energy greater than V. (The area under the curve in figure 1(a) has the units of power, I_0 is the beam current incident on the collector, and V_0 is the accelerating potential of the electron gun.) The rectangular outline OACD shown in figure 1(a) represents the monoenergetic electron beam launched from the electron gun; the area of the triangle BCE less that of DEF corresponds to the rf power produced by the

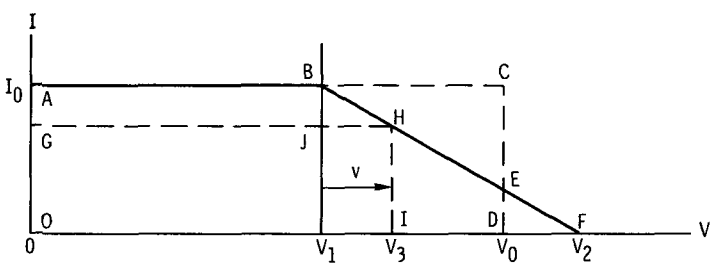

(a) Idealized current probability distribution function.

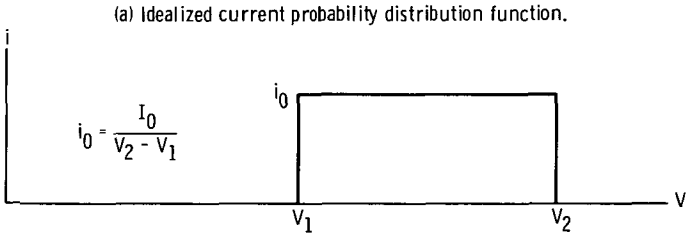

(b) Idealized current probability density function.

Figure 1. - Idealized current probability distribution and density functions.

tube. The probability density function shown in figure 1(b), which is the negative of the derivative of figure 1(a), describes the probability of finding electrons between the energies of V and $V + dV$ in the beam incident on the collector.

When secondary emission is neglected and all electrons in the beam are assumed to be directed axially, an opaque collector placed at V_3 will recover power from the beam equal to the area of the rectangle OGHI in figure 1(a). This area S may be written as

$$S = V_3 I = I(v + V_1) \tag{1}$$

The current intercepted at V_3 is

$$I = I_0 \frac{(V_2 - V_1 - v)}{V_2 - V_1} \tag{2}$$

The goal is to maximize S, the recovered power. By substituting equation (2) into (1) and differentiating with respect to v,

$$\frac{dS}{dv} = I_0 \frac{(V_2 - 2V_1 - 2v)}{V_2 - V_1} \tag{3}$$

Inspection shows that S increases for increasing v as long as $V_2 > 2V_1 + 2v$. Three conclusions result from equation (3):

(1) If $V_2 \leq 2V_1$, the maximum power is recovered when $v = 0$.

(2) If $V_2 > 2V_1$, the maximum power is recovered when

$$v = \frac{V_2 - 2V_1}{2} \tag{4}$$

(3) If $V_1 = 0$, that is if the probability density is constant up to V_2 or the probability distribution reduces to a triangle, the maximum power is recovered when

$$v = \frac{V_2}{2} \tag{5}$$

The remaining unrecovered power in the original triangular distribution is represented by the two triangles BJH and HIF, which are of equal area when equation (5) is fulfilled. The argument just described can be applied to the maximization of the re-

covery of the energy in any triangular distribution, including these. Additional collectors should be biased to be in the centers of the voltage intervals. It follows then from equation (5) that, for a triangular distribution function, the maximum power would be recovered by N collectors when they are equally spaced in voltage.

Collector Efficiency

The collector efficiency η_C may be defined as the ratio of the power recovered from the beam by the collector to the power contained in the beam as it is incident on the collector assembly. What follows is a derivation of this efficiency for a triangular distribution of current acted upon by a depressed collector of N stages equally spaced in potential. Both radial velocities and secondary emission are taken into account, and the generality of the result is discussed.

When N depressed stages are employed, current may be collected at N + 1 potentials, counting the tube body. The voltage increment between the depressed stages $V_{max}/(N + 1)$ is as shown in figure 2(a). For this model, equal currents are intercepted by each of the stages and the tube body. A fraction of the intercepted current C_f will fall on the leading edge of the collector; the resulting secondary emission will then be

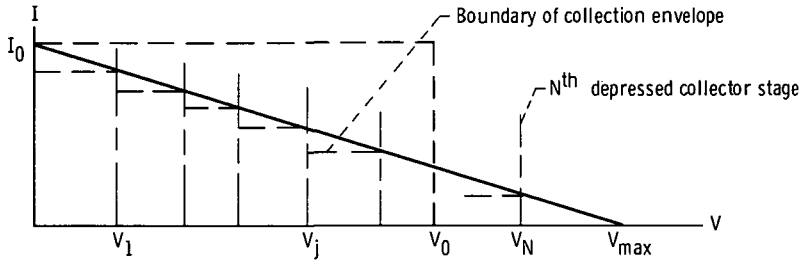

(a) Current probability distribution function with N depressed collector stages.

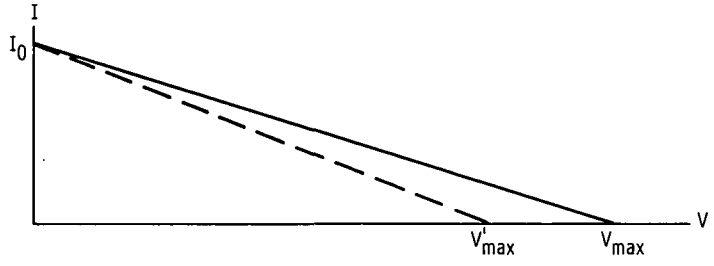

(b) Current probability distribution function for recoverable power.

Figure 2. - Idealized current probability distribution functions.

collected at the next least depressed stage. To accommodate this effect to the derivation, the term s is introduced where

$$s = C_f \gamma_0 \tag{6}$$

and the variation in secondary yield γ as a function of incident electron energy is neglected by taking γ_0, the maximum secondary yield.

The symbol p represents the power not included within the envelope of collection formed by each collector and can be written

$$p = \frac{I_0 V_{max}}{2(N + 1)^2} \tag{7}$$

Since the electrons intercepted by the N^{th} depressed stage will have an average energy midway between V_N and V_{max}, the beam power $P_{u(N)}$ which is not recovered from the current collected there can be written

$$P_{u(N)} = p(1 - \gamma_0) \tag{8}$$

Expression (8) is derived under the assumption that the N^{th} collector is opaque. The secondary emission from the N^{th} collector is intercepted on the $(N - 1)^{th}$ collector.

Similarly, the unrecovered power from the current collected at the successive stages in a system where $N > 2$ is

$$P_{u(N-1)} = p(1 - s + 3\gamma_0) \tag{9}$$

$$P_{u(j)} = p(1 + 2s) \tag{10}$$

where $1 \leq j < N - 1$.

At the tube body the unrecovered power becomes

$$P_{u(0)} = p(1 + 3s) \tag{11}$$

Assuming that the energy of the electron in excess of V_0 may be recovered, the total unrecovered power may then be expressed as

$$P_{uT} = p[N + 1 + 2\gamma_0 + 2s(N - 1)] \tag{12}$$

The power P_{Sb} remaining in the beam as it is incident on the collector assembly may be expressed in two different ways

$$P_{Sb} = I_0 V_0 (1 - \eta_0) \tag{13}$$

$$P_{Sb} = \frac{I_0 V_{max}}{2} \tag{14}$$

where η_0 is the conversion efficiency of the tube. In terms of figure 1(a), η_0 is the area of the triangle BCE less than of the triangle DEF, divided by $I_0 V_0$.

From the preceding it follows that V_{max} can be written as a function of V_0

$$V_{max} = 2V_0 (1 - \eta_0) \tag{15}$$

The collector efficiency η_C becomes

$$\eta_C = \frac{P_{Sb} - P_{uT}}{P_{Sb}} \tag{16}$$

Upon substitution of equations (12), (14), and (7) into equation (16), the expression for the collector efficiency emerges as

$$\eta_C = \frac{N^2 + N - 2\gamma_0 - 2s(N - 1)}{(N + 1)^2} \qquad N \geq 2 \tag{17}$$

When only one depressed collector stage is used, the collector efficiency reduces to

$$\eta_C = \frac{1 - \gamma_0}{2} \tag{18}$$

To allow for radial velocities, refer to figure 2(b). If the fraction η_r of the kinetic energy in the radially directed velocity component is assumed to be constant for all energies, a new probability distribution function of recoverable electron energy, represented by the dashed line, may be drawn. In this case,

$$V'_{max} = \frac{V_{max}}{1 + \eta_r} \tag{19}$$

For N collectors ($N \geq 2$) equally spaced by $V'_{max}/(N + 1)$ in potential, the unrecovered power and collector efficiency become

$$P_{uT} = \frac{p}{1 + \eta_r}\left[\eta_r(N + 1)^2 + N + 1 + 2\gamma_0 + 2s(N - 1)\right] \tag{20}$$

$$\eta_C = 1 - \frac{\eta_r}{1 + \eta_r} - \frac{N + 1 + 2\gamma_0 + 2s(N - 1)}{(1 + \eta_r)(N + 1)^2} \tag{21}$$

Although many practical current probability distributions are not triangular in shape, the expressions just derived have some application in many cases. In general, if a sufficient number of collectors are used, the areas of unrecovered power will be approximately triangular. Then if v_j and i_j are, respectively, the potential increment and the intercepted current for the j^{th} collector stage, the unrecovered power can be expressed as

$$P_{uT} = \frac{1}{2}\sum_{j=0}^{N} v_j i_j \tag{22}$$

where

$$V_{max} = \sum_{j=0}^{N} v_j \tag{23}$$

and

$$I_0 = \sum_{j=0}^{N} i_j \tag{24}$$

If the stages are chosen so that the intercepted currents i_j are all equal, the unrecovered power is

$$P_{uT} = \frac{I_0}{2(N+1)} \sum_{j=0}^{N} v_j = \frac{I_0 V_{max}}{2(N+1)} \tag{25}$$

Equation (25) is identical to equation (20) with s, γ_0, and η_r set at zero.

Equation (16) still applies to the collector efficiency. However, V_{max} is not related to V_0 in the same way as in equation (15), and the inclusion of secondary emission in the analysis is complicated by the nonuniformity in magnitude of the v_j's. When a detailed current distribution is known, the preceding analysis can be carried out. Such a calculation is described elsewhere in this report but is not as readily adapted to a simple analytical expression as the triangular distribution.

Before leaving the subject of collector efficiency a comment should be made regarding enhancement of the secondary yield due to grazing angles of incidence at the collector. Figure 3(a) conveys a representation of the problem of the electron moving at an angle φ from the axial direction and striking the collector plate at an angle of incidence α. The collector plate is shown as a flat plane at angle β to the normal to the tube axis.

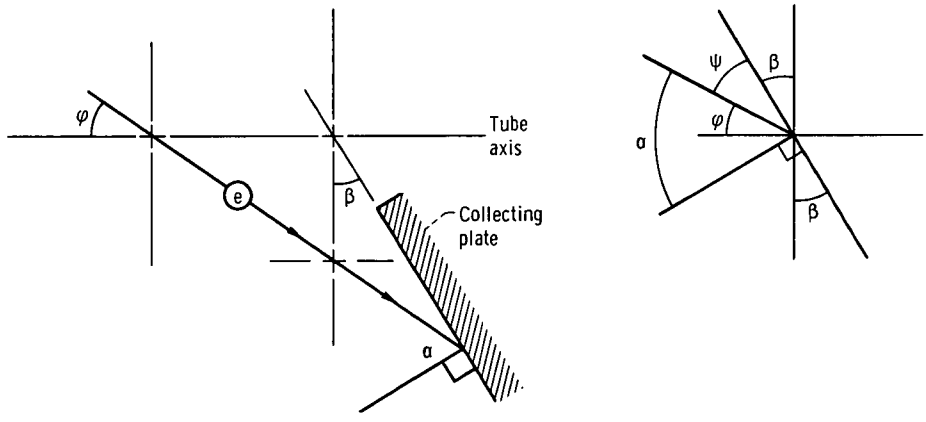

(a) Representation of electron moving at angle φ from axial direction and striking collector plate at angle of incidence α.

(b) Diagram of figure 3(a) translated to a single intersection.

Figure 3. - Electron at grazing angle of incidence.

The diagram of figure 3(a) is translated to a single intersection in figure 3(b). By inspection, the following equations can be written:

$$\psi = 90^{\circ} - \alpha \tag{26}$$

$$\varphi + \psi + \beta = 90^{\circ} \tag{27}$$

By subtracting equation (26) from (27) the angle of incidence is found to be

$$\alpha = \varphi + \beta \tag{28}$$

The angle β is known from the tube design. The angle φ can be computed by using the expression

$$\varphi = \sin^{-1}\left(\eta_r^{1/2}\right) \tag{29}$$

The effective secondary yield γ_e, increased by the effect of the grazing angle of incidence, then becomes (ref. 5)

$$\gamma_e = \frac{\gamma_0}{\cos(\varphi + \beta)} \tag{30}$$

An expression for the overall tube efficiency η_t may be developed, based on the collector efficiency. Two other loss mechanisms must be considered, the microwave efficiency η_{RF} within the tube and the fraction $\mathscr{L}$ of the electron beam power which is intercepted by the tube body and, therefore, is not incident on the collector assembly.

$$\eta_t = \frac{\eta_0 \eta_{RF}}{1 - (1 - \eta_0)\eta_C + \mathscr{L}} \tag{31}$$

If no depressed collector stages are used, equation (31) reduces to

$$\eta_{tz} = \frac{\eta_0 \eta_{RF}}{1 + \mathscr{L}} \tag{32}$$

where η_{tz} is the tube efficiency for a collector efficiency of zero and negligible heater power.

POWER LOSSES IN THE DIRECT-CURRENT POWER SUPPLY

Rectifier Losses

In considering the microwave tube as part of an electrical system, it is necessary to analyze the operation of the dc supply that powers the tube. Losses in the system for a

typical operation are described in figure 4(a), and the nominal circuit diagram is shown in figure 4(b).

The power supply consists of a parallel converter driven by transistor switches, a single toroidal transformer with multiple secondary windings, and full-wave rectification. This arrangement is not presented as being the best circuit for every application, but one for which efficiency can be readily computed. The systems employed in operational satellites are generally more sophisticated.

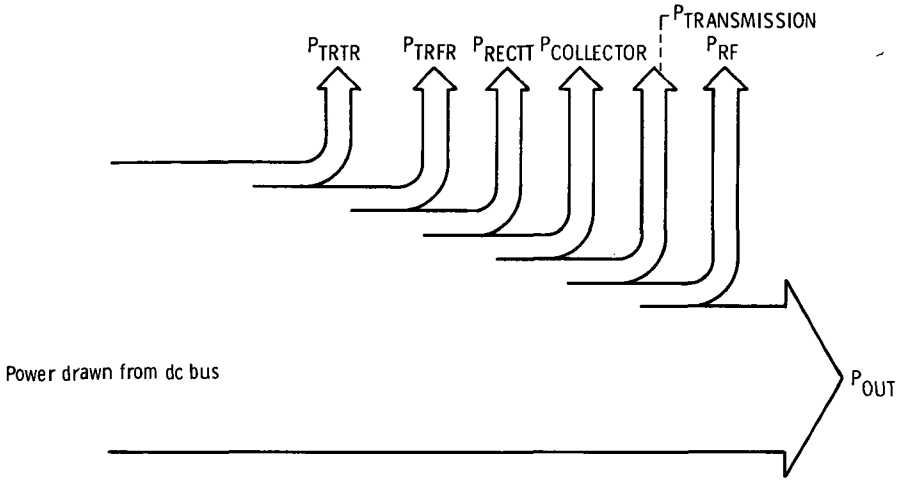

(a) Power flow diagram.

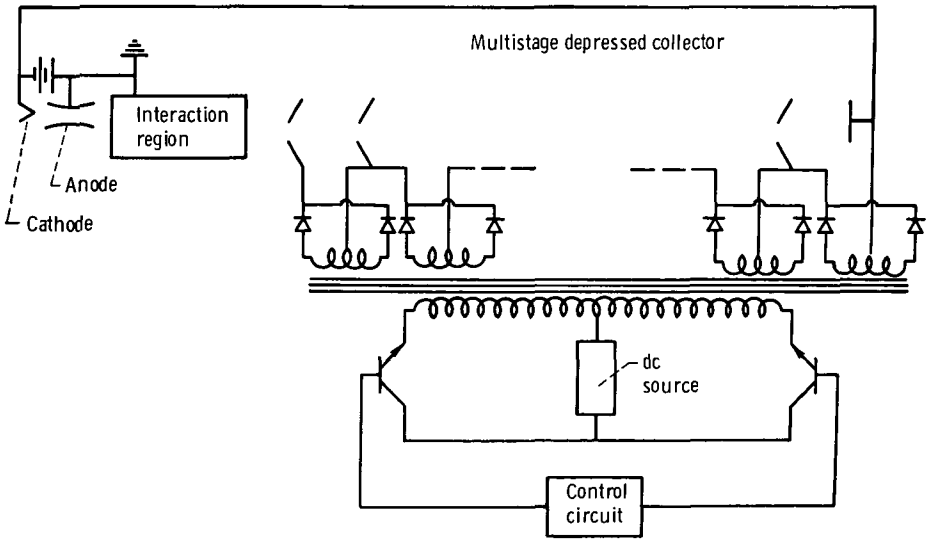

(b) Nominal circuit diagram for power supply.

Figure 4. - Power flow and power supply circuit diagrams.

The power lost as a result of beam interception at the anode and the interaction region is supplied by the collector power supply in this calculation. As shown in figure 4(b), this current would be delivered by the cathode supply in a practical circuit. However, to simplify the calculation of system efficiency, a separate power supply for the cathode was not included. Little error should be introduced since only a few percent of the beam current is intercepted and the cathode supply efficiency should be within a few percent of the collector supply efficiency.

The power losses in the rectifiers P_{RECT} are caused by forward conduction and reverse leakage. For a full-wave rectifier circuit with a center-tapped transformer secondary which is conducting a current I at a square-wave peak voltage of V

$$P_{RECT} = \frac{N_R I^2 V_{FM}}{I_{FM}} + \frac{4V^2 I_{RM}}{N_R V_{RM}} \tag{33}$$

where N_R is the number of rectifiers in series, V_{FM} is the forward voltage drop at maximum rated current, I_{FM} is the maximum rated forward current, V_{RM} is the maximum rated reverse rectifier voltage drop, and I_{RM} is the reverse current at the maximum rated reverse voltage.

For each collector a separate pair of rectifiers must be employed. The total of all the rectifier losses is P_{RECTT}.

Transformer Losses

The power output from the transformer can be computed by using the foregoing expressions, but the power input cannot be computed without first finding the transformer efficiency. The efficiency can be computed by using the equations derived in this section for a transformer which is supplying the approximate power required. Since transformer losses vary as the fourth root of the power handled, only a small error is introduced by then using this efficiency to compute the transformer losses and the power input to the transformer.

The transformer losses in the power supply are estimated by assuming that one toroidal transformer is used. The transformer is center tapped in the primary winding. The secondary consists of a separate, center-tapped winding for each collector. Leakage reactance and capacitance are neglected. The maximum current I_{SM} in any of the legs of the secondary winding is

$$I_{SM} = \frac{P_{OUT}}{\eta_{tz} V_0} \tag{34}$$

If we neglect for a moment the losses in the rectifiers and transformer, the primary current I_P, is

$$I_P = \frac{P_{OUT}}{\eta_t V_P} \tag{35}$$

where V_P is the input dc voltage.

If the entire secondary winding is designed to carry I_{SM} and the rated current density is the same for primary and secondary, then

$$A_1 = \frac{\eta_{tz} V_0 A_2}{\eta_t V_P} \tag{36}$$

where A_1 and A_2 are the cross-sectional areas of the conducting portions of the primary and secondary windings, respectively.

The basic relation needed for the transformer analysis is Faraday's law

$$N_P = \frac{V_P}{4 W_f f B_M A_c} \tag{37}$$

where N_P is the number of turns in the primary winding, W_f is the waveform factor, f is the frequency, B_M is the magnetic flux density, and A_c is the cross-sectional area of the iron core.

The transformer windings will fill a fraction F of the toroidal window A_w

$$A_w F = 2(A_1 N_P + A_2 N_S)(1 + W_{in}) \tag{38}$$

where W_{in} is the fraction of increase in the cross-sectional area of the conductors caused by insulation.

The cross-sectional areas of the two windings can now be written

$$A_1 = \frac{A_w F}{2 N_P \left(1 + \frac{\eta_t}{\eta_{tz}}\right)(1 + W_{in})} \tag{39}$$

$$A_2 = \frac{A_w F}{2N_S \left(1 + \frac{\eta_{tz}}{\eta_t}\right)(1 + W_{in})} \tag{40}$$

The fraction F_1 of the toroidal window filled by the primary winding is

$$F_1 = \frac{F}{1 + \frac{\eta_t}{\eta_{tz}}} \tag{41}$$

Drawing upon an earlier result (ref. 6) the approximate lengths of the primary and secondary windings, L_1 and L_2, respectively, are known to be

$$L_1 = 2N_P\left[2H_T + D_{OT} + D_{IT}\left(1 - 2\sqrt{1 - F_1}\right)\right] \tag{42}$$

$$L_2 = 2N_S\left[2H_T + D_{OT} + D_{IT}\left(3 - 2\sqrt{1 - F_1} - 2\sqrt{1 - F}\right)\right] \tag{43}$$

where H_T is the height, D_{OT} is the outside diameter, and D_{IT} is the inside diameter of the core box.

The conduction losses P_{Cu} in the windings can be written now, considering that only one-half of each coil is excited at a time and that the length of wire between taps in the secondary is proportional to the fraction of the secondary voltage developed.

$$P_{Cu} = \frac{I_P^2 L_1 \rho}{2A_1} + \sum_{j=0}^{N} \frac{I_{Sj}^2 \rho L_2 \, \Delta V_{Sj}}{2A_2 V_0} \tag{44}$$

where I_{Sj} is the current carried by the j^{th} segment of the secondary, ΔV_{Sj} is the voltage built up on the j^{th} winding, and ρ is the resistivity of the winding material, which is assumed to be at a uniform temperature.

It has been shown previously (ref. 7) that, for a toroidal transformer with a core having given ratios of inner to outer diameter Y and height to buildup Z, the most efficient design is obtained when the height H_M of the iron core is given by

$$H_M = \left(\frac{5k_1}{3k_2}\right)^{1/8} \tag{45}$$

where k_1 and k_2 are defined in the expression for transformer efficiency η_{TRFR} and are related to the conduction and iron losses, respectively.

$$\eta_{TRFR} = 100 - k_1 H_M^{-5} - k_2 H_M^3 \tag{46}$$

The function k_1 may be derived from equation (44) by the same procedure as used in reference 7 and is

$$k_1 = \frac{100\rho Z^2(1 + W_{in})G}{2\pi(0.85)^2 F f^2 B_M^2 \left[\frac{2Y}{Z(1 - Y)} - 0.1\right]^2 V_P I_P W_f^2} \tag{47}$$

where

$$G = V_P^2 I_P^2 \left(1 + \frac{\eta_t}{\eta_{tz}}\right)\left[2.2 + 0.2X_A + \frac{2}{Z(1 - Y)}(1 + Y - 2YX_A)\right]$$

$$+ V_0 \left(1 + \frac{\eta_{tz}}{\eta_t}\right)\left[2 + 0.2X_A + 0.2X_B + \frac{2}{Z(1 - Y)}(1 + 3Y - 2YX_A - 2YX_B)\right] \sum_{j=0}^{N} I_{Sj}^2 \Delta V_{2j} \tag{48}$$

$$X_A = \sqrt{1 - F_1} \tag{49}$$

and

$$X_B = \sqrt{1 - F} \tag{50}$$

The function k_2 has been derived in reference 7

$$k_2 = \frac{100\pi\rho_M W_i f B_M}{V_P I_P}\left(\frac{1 + Y}{1 - Y}\right)\left(\frac{1}{Z^2}\right) \tag{51}$$

where ρ_M is the density of the core material and W_i is the core loss per unit mass, magnetic flux density, and frequency. The transformer losses may then be estimated by using equation (46).

Transistor Losses

The current I_{in}, which must be handled by the switching transistors, can now be computed including rectifier and transformer losses

$$I_{in} = \frac{\frac{P_{OUT}}{\eta_t} + P_{RECTT}}{V_P \eta_{TRFR}} \tag{52}$$

The number N_T of switching transistors which must be operated in parallel is determined so that they carry no more than one-half their rated current. It is assumed that the paralleled transistors will share the current equally. The power P_{TRTR} consumed by the switching transistors is (ref. 8)

$$P_{TRTR} \simeq N_T \left\{ \left[\left(\frac{I_{in}}{N_T} \right)^2 \frac{V_{SATR}}{I_{SATR}} + 2V_P I_{RT} \right] (1 - f\tau_s) + \frac{2V_P I_{in} f \tau_s}{3N_T} + I_B V_B \right\} \tag{53}$$

where V_{SATR} is the saturation voltage at rated current, I_{SATR} is the rated saturation current, I_{RT} is the reverse current, τ_s is the total switching time, I_B is the base current, and V_B is the base voltage.

In addition to the transistor, transformer, and rectifier losses just described, the control and regulation circuits associated with the power supply will consume about 5 percent of the power being conditioned in a typical converter system (ref. 9).

ESTIMATION OF EFFICIENCY FROM COMPUTED ELECTRON CURRENT DISTRIBUTION

The analysis described in the previous section has been applied to the current probability distribution for saturated operation computed for a 2-kilowatt traveling wave tube and shown in figure 5 (unpublished result from O. G. Sauseng). This distribution is vaguely similar to that shown in figure 1(a), and the placement of the first depressed collector stage was determined approximately from the criterion of equation (4). Successive stages were placed so as to maximize the intercepted area under the current distribution curve, but no stage is placed at a potential greater than V_0 since this energy is not readily recovered. Since figure 5 does not take radial velocity components into account, the potentials actually applied to the collectors are reduced from those shown as

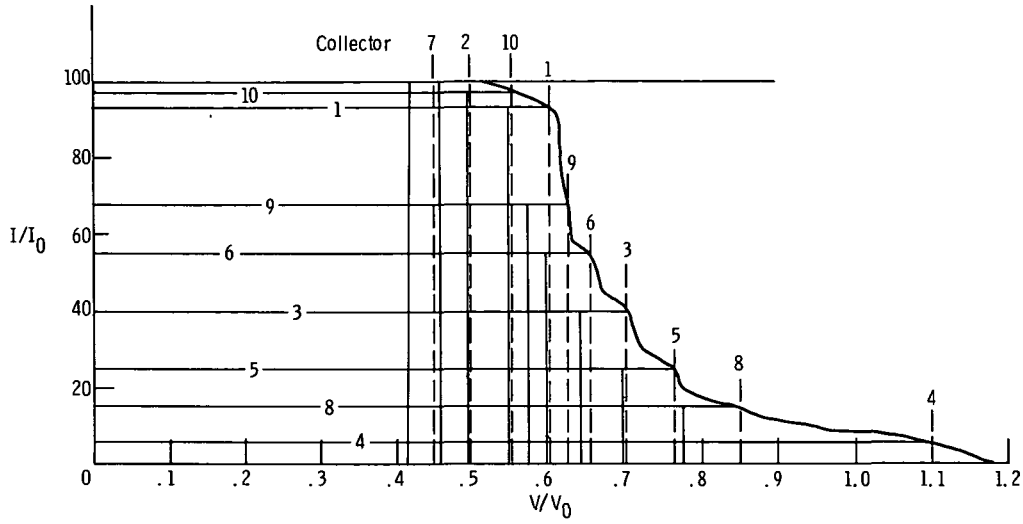

Figure 5. - Analysis of current probability distribution for saturated operation of a 2-kilowatt traveling wave tube. (Collector numbers denote order in which they were added to assembly.)

dashed lines by dividing by $1 + \eta_r$ and are shown as solid lines. The numbers assigned to the collectors denote the order in which they were added to the assembly.

The current probability distribution for the same tube operated at 12.0 decibels below saturation is shown in figure 6. The collector potentials chosen with the purpose of maximizing the tube efficiency for operation at saturation are also shown in the figure. With the tube operating below saturation, the electrons in the spent beam have a higher average velocity and are not collected with maximum efficiency. It would be possible to bias the collectors so that the collector efficiency would be very high for low rf power levels, but this would correspondingly reduce the efficiency at saturation.

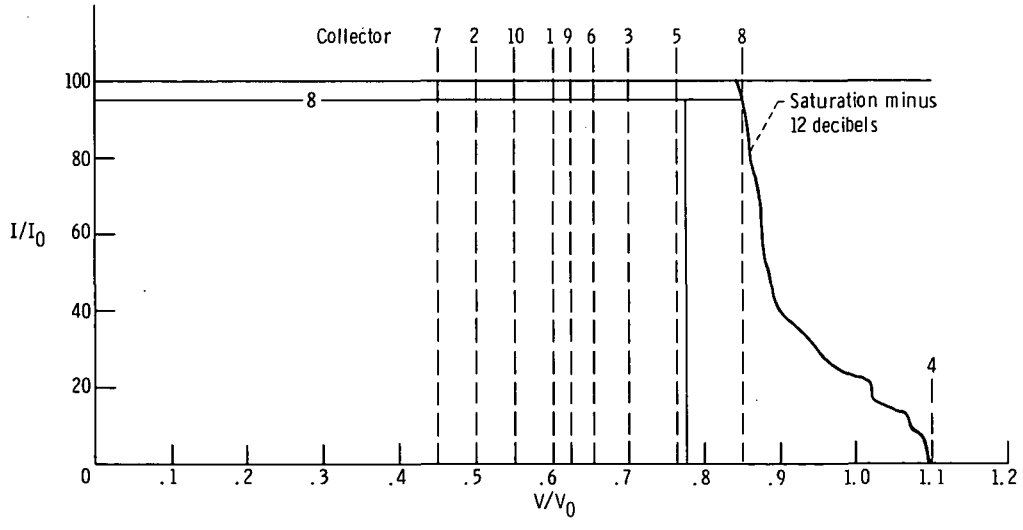

Figure 6. - Analysis of current probability distribution for a 2-kilowatt traveling wave tube operated at 12 decibels below saturation. (Collector numbers denote order in which they were added to assembly.)

The voltages and intercepted currents obtained from figures 5 and 6 have been used as the starting point for a calculation of the efficiencies of the collector, the tube, and the power supply based on the analytical development in the previous section of the report. The basic electronic efficiency of the tube is also obtained from figures 5 and 6. For operation at saturation, η_0 is 28.27 percent; and at 12 decibels below saturation, it is 7.55 percent. Power output is 534 watts when the input power is 12 decibels below saturation. The following assumptions are made: rf efficiency, 95 percent; transmission loss, 2 percent; and heater power, 7 watts. A computer program was written to expedite these calculations and to facilitate the study of the effects of the variation of some of the parameters.

For a typical collector design the average angle β described in figure 3 is approximately 18°. If $\eta_r = 0.1$, then from equations (29) and (30) $\gamma_e = 1.244\ \gamma_0$. For a collector coated with lampblack, γ_0 is 0.5 (measured by John Ferrante of Lewis using a low-energy-electron-diffraction, Auger emission spectroscopy system) so that $\gamma_e = 0.622$. By making an assumption about C_f, the efficiencies of the collector, the tube, and the entire system can be calculated and plotted as shown in figure 7. It can be seen that tube efficiency is markedly improved for the first few stages of depressed collectors added but increases only about 1 percent for each of the later stages. All losses in the power supply were computed or estimated in determining the system efficiency.

The biasing of the collector plates has been determined solely to maximize efficiency for operation at saturation; as a result, it can be seen in figure 6 that at operation 12 decibels below saturation some of the collectors do not influence the distribution of collector currents. This explains the reduction in collector efficiency and the stepped dis-

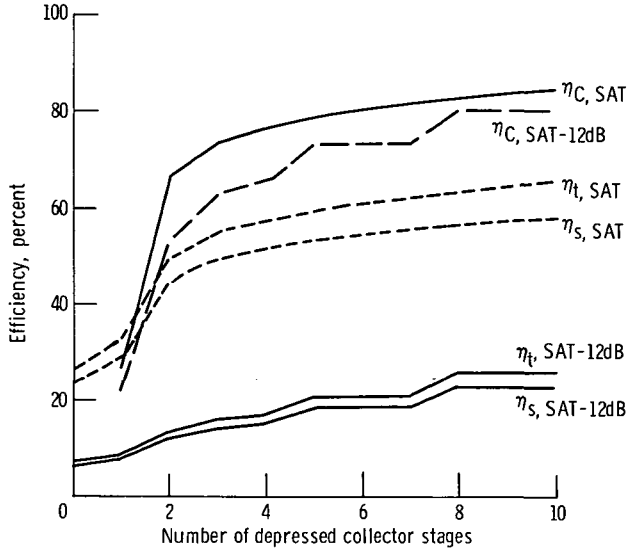

Figure 7. - Efficiencies of collector, tube, and entire system.

continuities in the curves in some of the figures for operation at 12 decibels below saturation.

At a sacrifice of efficiency at full-power output, the collector efficiency below saturation could be improved by a rearrangement of the collectors. Because the current probability distribution becomes more nearly a rectangle, collector efficiency could be increased the further operation is from saturation.

The effect on collector efficiency of a change in C_f is illustrated in figure 8 for the case where $\gamma_e = 0.622$. When only 10 percent of the current is collected on the leading edges of the collectors, the efficiency is greater than for equal distribution but the difference is only about 4 percent at most. As the number of collectors is increased the difference becomes smaller.

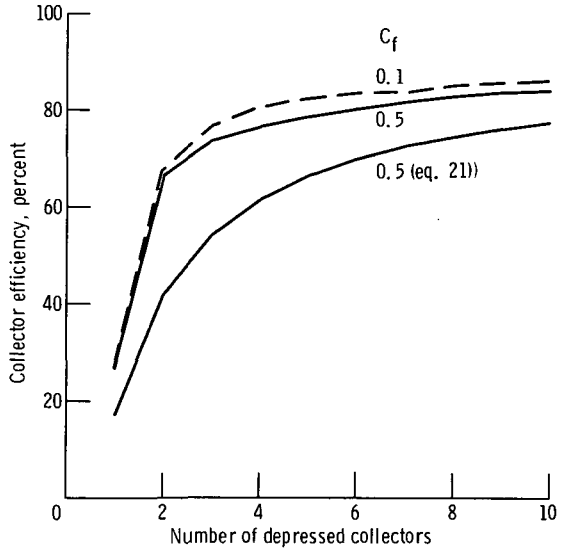

Figure 8. - Effect on collector efficiency of change in fraction of intercepted current incident on leading edge of collector C_f.

Also plotted in figure 8 is the analytical expression for collector efficiency presented in equation (21). This expression was derived for conditions which do not apply to the other curves in the figure. However, as the number of depressed stages is increased, the current and voltage increments become more nearly equal and the areas of the probability distribution not within the collection envelope become more triangular in shape. Thus, equation (21) becomes a better approximation to the collector efficiency, and the separation of the curves is reduced. If nothing were known about the current probability distribution function, equation (21) might be used to approximate collector efficiency.

The total power input to the system is plotted in figure 9 as a function of the number

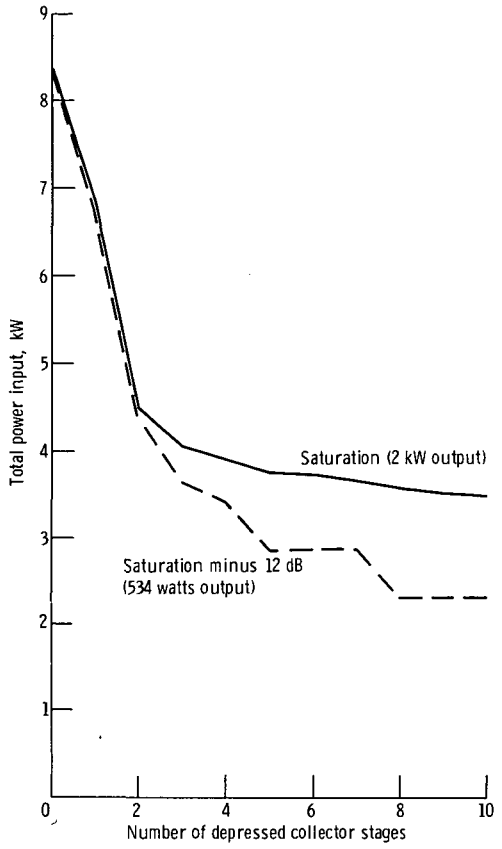

Figure 9. - Total power input to system as function of number of depressed collector stages.

of depressed collector stages for operation at saturation and at 12 decibels below saturation. All losses in the system, the power delivered to the cathode heater, and an allowance of 5 percent for filters and regulation circuits, as well as the computed power dissipation in the tube, transformer, transistors, and rectifiers, are included. Note that with no depressed collector stages the system consumes the same power regardless of the rf input power.

The power supply calculations are based on the following conditions: magnetic materials, Supermendur (refs. 10 and 11); transformer windings, copper; transformer operating temperature, 200° C; excitation, square wave; maximum magnetic flux density, 1.8 T; frequency, 800 Hz; V_1, 28 V; fill factor, 50 percent; coil insulation area, 12.5 percent; core inside to outside diameter ratio, Y, 0.8; core height to buildup ratio, Z, 1.0; transistors, type 1401; and silicon rectifiers (ref. 12).

The transformer efficiency relation was solved for a matrix of values of Y and Z, and the values of 0.8 and 1.0 were chosen because maximum efficiency was achieved in this neighborhood under a variety of conditions. No attempt was made to solve for the most efficient transformer design (ref. 7) for each case.

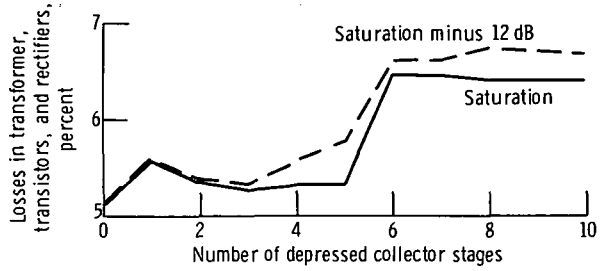

Figure 10. - Losses in system as function of number of depressed collector stages.

The penalty paid by the power supply in increased losses as the system is complicated by more stages of depressed collectors is illustrated in figure 10. Only the calculated losses in the transformer, transistors, and rectifiers are included herein. From none to six collectors, the system efficiency is reduced overall about 1 percent, mostly because of the decreased transformer efficiency. After six stages, the decreases in transformer efficiency are approximately offset by increases in transistor efficiency.

CONCLUSIONS

The collector and tube efficiencies for a microwave tube with a multistage depressed collector have been calculated in two ways. First, an analytical expression was derived based on a hypothetical triangular current probability distribution at the collector. The effects of secondary emission and radial velocity components on the collector efficiency are included in this analysis. The second calculation is based on the current probability distribution determined analytically for a specific tube design; a digital computer was used to perform the detailed calculations required.

Even though these two calculations are based on quite different current distributions, the two results differ by less than 10 percent when 10 stages of depressed collection are considered. When nothing is known of the actual current distribution in the tube, the analytical expression probably provides a satisfactory estimate of the collector efficiency.

An estimate is made of the efficiency of the power supply required to drive the traveling wave tube equipped with a multistage depressed collector. The power supply described herein is a simple parallel inverter employing transistor switching, a single toroidal transformer with multiple secondary windings, and full-wave rectification. Losses in the filter and regulation circuits are estimated from a recently published system design. An actual power supply for this application might be quite different than the simple system described in the text and incorporated in the computer program.

From the results, it can be seen that the first few stages of depressed collection im-

prove the tube efficiency substantially, but that after the sixth stage, tube efficiency improves only about 1 percentage point for each additional stage.

Lewis Research Center,
National Aeronautics and Space Administration,
Cleveland, Ohio, August 14, 1972,
682-10.

APPENDIX - SYMBOLS

A_c cross-sectional area of transformer core, m^2

A_w area of window of core box, m^2

A_1 cross-sectional area of conducting portion of primary winding of transformer, m^2

A_2 cross-sectional area of conducting portion of secondary winding of transformer, m^2

B_m maximum magnetic flux density, T

C_f fraction of intercepted current incident on leading edge of collector

D_{IT} inside diameter of core box, m

D_{OT} outside diameter of core box, m

F transformer fill factor

F_1 primary winding fill factor

f frequency, Hz

G function defined by eq. (48)

H_m height of magnetic core for maximum transformer efficiency, m

H_T height of core box, m

I current defined by fig. 1(a), A

I_B transistor base current, A

I_{FM} maximum forward rated rectifier current, A

I_{in} current drawn from dc source, A

I_P primary winding current, A

I_{RM} reverse current at maximum rated rectifier inverse voltage, A

I_{RT} reverse transistor current, A

I_{SATR} rated transistor saturation current, A

I_{Sj} current carried by the j^{th} segment of secondary, A

I_{SM} maximum secondary winding current, A

I_0 beam current incident on collector, A

i_j current intercepted by j^{th} collector stage, A

k_1 function defined by eq. (47)

k_2	function defined by eq. (51)
$\mathscr{L}$	fraction of beam current intercepted by tube body
L_1	length of primary winding, m
L_2	length of secondary winding, m
N	number of stages of depressed collectors
N_P	number of primary turns in transformer
N_R	number of rectifiers connected in series
N_S	number of secondary turns in transformer
N_T	number of switching transistors connected in parallel
$P_{COLLECTOR}$	power dissipated in the collector, W
P_{Cu}	copper losses in transformer, W
P_{OUT}	radiofrequency output power from tube, W
P_{RF}	power dissipated by electromagnetic waves in slow wave structure, W
P_{RECT}	power dissipated in one pair of power rectifiers, W
P_{RECTT}	power dissipated in all of the rectifiers of the power supply, W
$P_{TRANSMISSION}$	power lost from electron beam in transmission through tube, W
P_{TRFR}	power dissipated in the transformer, W
P_{TRTR}	power dissipated in transistors, W
P_{Sb}	power in electron beam incident on collector, W
$P_{u(j)}$	unrecovered power from electrons collected at j^{th} collector, W
P_{uT}	total unrecovered power, W
p	function defined by eq. (7)
S	area intercepted by collector at V_3 in fig. 1(a)
s	function defined by eq. (6)
V_B	transistor base voltage, V
V_{FM}	rectifier forward voltage drop at rated current, V
V_{max}	maximum energy of electrons in spent beam, V
V'_{max}	maximum energy of electrons in spent beam corrected for radial velocities, V

V_N voltage applied to N^{th} collector stage, V

V_P transformer maximum primary voltage, V

V_{RM} maximum rated reverse rectifier voltage, V

V_{SATR} transistor saturation voltage at rated current, V

ΔV_{Sj} secondary voltage built up between taps on j^{th} increment, V

V_0 beam voltage, V

V_1 voltage defined in fig. 1, V

V_2 voltage defined in fig. 1, V

V_3 voltage defined in fig. 1, V

v voltage defined in fig. 1, V

v_j voltage between collector stages j and j + 1, V

W_f waveform factor

W_i core loss, W/(kg)(T)(Hz)

W_{in} fraction of increase in cross-sectional area of transformer windings due to insulation

X_A function defined by eq. (49)

X_B function defined by eq. (50)

Y ratio of inner to outer diameter of magnetic core

Z ratio of height to buildup of the magnetic core

α angle of incidence for electron striking forward face of collector plate

β angle collector plate makes with tube axis

γ_e effective secondary electron yield

γ_0 maximum secondary yield for normal incidence

η_C collector efficiency

η_{RF} radiofrequency efficiency of tube

η_r fraction of beam energy due to radially directed component of electron velocity

η_s total system efficiency for tube and power supply

η_{TRFR} transformer efficiency

η_t overall tube efficiency, neglecting heater power

η_{tz} tube efficiency with no depressed collector stages, neglecting heater power

η_0 electronic conversion efficiency of tube

ρ resistivity of transformer winding material, Ω - m

ρ_M mass density of transformer magnetic material, kg/m^3

τ_s transistor switching time, sec

φ angle which electron incident on forward face of collector makes with axis of tube

ψ angle defined by fig. 3

Subscript:

TRTR transistor

REFERENCES

1. Kosmahl, Henry G.: A Novel, Axisymmetric, Electrostatic Collector for Linear Beam Microwave Tubes. NASA TN D-6093, 1971.

2. Kavanagh, Francis E.; Alexovich, Robert E.; and Chomos, Gerald J.: Evaluation of Novel Depressed Collector for Linear-Beam Microwave Tubes. NASA TM X-2322, 1971.

3. Neugebauer, Wendell; and Mihran, Theodore G.: A Ten-Stage Electrostatic Depressed Collector for Improving Klystron Efficiency. IEEE Trans. on Electron Devices, vol. ED-19, no. 1, Jan. 1972, pp. 111-121.

4. Okoshi, Takanori; Chiu, Eng-Beng; and Matsuki, Sadao: The Tilted Electric Field Soft-Landing Collector and Its Application to a Traveling-Wave Tube. IEEE Trans. on Electron Devices, vol. ED-19, no. 1, Jan. 1972, pp. 104-110.

5. Kaminsky, Manfred: Atomic and Ionic Impact Phenomena on Metal Surfaces. Academic Press, 1965.

6. Dayton, James A., Jr.: Toroidal Transformer Design Program with Application to Inverter Circuitry. NASA TM X-2540, 1972.

7. Dayton, James A., Jr.: Design of Toroidal Transformers for Maximum Efficiency. NASA TM X-2539, 1972.

8. Anon.: RCA Power Circuits DC to Microwave. Tech. Series SP-51, RCA Electronics Components Div., Harrison, N. J., p. 139.

9. Gourash, Francis; Birchenough, Arthur G.; Pittman, Paul F.; Ravas, Richard J.; and Hall, William G.: Development and Performance of Pulse-Width-Modulated Static Inverter and Converter Modules. NASA TN D-6511, 1971.

10. Gould, H. L. B.; and Wenny, D. H.: Supermendur, A New Rectangular-Loop Magnetic Material. Elect. Eng., vol. 76, no. 3, Mar. 1957, pp. 208-211.

11. Frost, R. M.; McVay, R. E.; and Pavlovic, D. M.: Evaluation of Magnetic Materials for Static Inverters and Converters. NASA CR-1226, 1969.

12. Anon.: RCA Transistor, Thyristor, and Diode Manual. Tech. Series SC-14, RCA Electronics Components Div., Harrison, N. J., 1969, pp. 558-560.

NATIONAL AERONAUTICS AND SPACE ADMINISTRATION
WASHINGTON, D.C. 20546

OFFICIAL BUSINESS
PENALTY FOR PRIVATE USE $300

SPECIAL FOURTH-CLASS RATE
BOOK

POSTAGE AND FEES PAID
NATIONAL AERONAUTICS AND
SPACE ADMINISTRATION
451

U.S.MAIL

POSTMASTER: If Undeliverable (Section 158 Postal Manual) Do Not Return

"The aeronautical and space activities of the United States shall be conducted so as to contribute . . . to the expansion of human knowledge of phenomena in the atmosphere and space. The Administration shall provide for the widest practicable and appropriate dissemination of information concerning its activities and the results thereof."

—NATIONAL AERONAUTICS AND SPACE ACT OF 1958

NASA SCIENTIFIC AND TECHNICAL PUBLICATIONS

TECHNICAL REPORTS: Scientific and technical information considered important, complete, and a lasting contribution to existing knowledge.

TECHNICAL NOTES: Information less broad in scope but nevertheless of importance as a contribution to existing knowledge.

TECHNICAL MEMORANDUMS: Information receiving limited distribution because of preliminary data, security classification, or other reasons. Also includes conference proceedings with either limited or unlimited distribution.

CONTRACTOR REPORTS: Scientific and technical information generated under a NASA contract or grant and considered an important contribution to existing knowledge.

TECHNICAL TRANSLATIONS: Information published in a foreign language considered to merit NASA distribution in English.

SPECIAL PUBLICATIONS: Information derived from or of value to NASA activities. Publications include final reports of major projects, monographs, data compilations, handbooks, sourcebooks, and special bibliographies.

TECHNOLOGY UTILIZATION PUBLICATIONS: Information on technology used by NASA that may be of particular interest in commercial and other non-aerospace applications. Publications include Tech Briefs, Technology Utilization Reports and Technology Surveys.

Details on the availability of these publications may be obtained from:

SCIENTIFIC AND TECHNICAL INFORMATION OFFICE

NATIONAL AERONAUTICS AND SPACE ADMINISTRATION

Washington, D.C. 20546